

Complex scaling spectrum using multiple avoided crossings at stabilization graph

Petra Ruth Kaprálková-Žďánská¹

¹ *Department of Radiation and Chemical Physics, Institute of Physics, Academy of Sciences of the Czech Republic, Na Slovance 2, 182 21 Prague 8, Czech Republic*

(*Electronic mail: kapralova@fzu.cz)

(Dated: 7 December 2021)

This study concerns finite basis set $\{\chi_k\}$ calculations of resonances based on real scaling, $\chi_k(x) \rightarrow \chi_k(xe^{-\eta})$. I demonstrate that resonance width is generally influenced by *several* neighboring quasi-discrete continuum states. Based on this finding I propose a new method to calculate the complex resonance energy together with several states of complex rotated continuum. The theory is introduced for a one-dimensional model, then it is applied for helium doubly excited resonance $2s^2$. The new method requires the real spectrum (“stabilization graph”) for a sufficiently large interval of the parameter η on which the potential curve of the sought resonance gradually meets several different quasi-continuum states. Diabatic Hamiltonian which comprehends the resonance and the several quasi-continuum states participating at the avoided crossings is constructed. As η is taken to complex plane, $\eta \rightarrow i\theta$, the corresponding part of the complex scaled spectrum is obtained.

I. INTRODUCTION

Resonance state represents quantum particle which is temporarily trapped within a confined space therefore resonance wavefunction resembles bound state wavefunction with an outgoing wave¹. The norm of the captured quantum particle drops down in time according to the first order kinetics, which inherently brings about a diverging character of the outgoing wave and also explains complex energy eigenvalue of resonance state with imaginary part given by half decay rate². Wherefore resonances do not belong to \mathcal{L}^2 space.

Different computational approaches to calculate resonances (auto-ionizing states) have been developed. Perhaps the most famous method is represented by *complex scaling*^{3,4} and *exterior complex scaling*⁵⁻⁸ of Hamiltonian (or interchangeably basis set), which effectively transforms resonances onto \mathcal{L}^2 space. These methods enable to construct non-Hermitian Hamiltonian which provides complex energies of resonances and rotated continuum.

Another approach to resonances is represented by *stabilization methods*. These methods are often used for ab initio calculations of molecular resonances as their main advantage is that they rely on Hermitian calculations. Resonances are derived from real energies obtained for states above ionization threshold, namely from *stabilization graph*, which is represented by above-threshold potential energy curves obtained as the problem is parametrized in various ways, e.g. real scaling of the basis set⁹⁻¹¹, or adding a binding potential¹²⁻¹⁴. Complex resonance energies are obtained via extrapolation of the free parameter to complex plane.

Yet another method, popular for its relatively simple implementation to quantum chemistry packages, is represented by *complex absorbing potential*¹⁵⁻¹⁸. Basic idea here is enforcing outgoing boundary conditions via additional artificial imaginary potential term which is localized in the asymptotic region.

Apart of these three types of methods, there are also approaches based on projection operators¹⁹, scattering the-

ory²⁰⁻²³, or Siegert state expansion²⁴ available to calculate resonances.

In this paper I propose a new method with the unique feature to calculate partial complex scaling spectrum, *resonances and rotated continuum*, using stabilization graph. The ability to calculate discretized rotated continuum is important for a subsequent implementation of strong field interactions²⁵⁻²⁷. Future intended use of the proposed method is particularly for ab initio simulations of laser-atom interactions phenomena such as high-order harmonics generation using standard quantum chemistry packages. The paper is organized as follows.

First, in Section II, I discuss the relationship between stabilization method, complex coordinate scaling, and complex absorbing potential, where the argument is backed up by illustrative calculations for a one-dimensional model potential. It is shown that avoided crossings found at stabilization graph continue to complex plane of the free parameter, where they end up in exceptional points (EPs)¹¹. Such EPs designate transition between adiabatic and diabatic regimes where resonance decouples from quasi-continuum states.

In Section III, I suggest a diabatic Hamiltonian for a *set* of avoided crossings in the stabilization graph, where the diabatic states include the resonance state defined by constant real energy, and several close states of discretized continuum, which are analytically dependent on the free real parameter (here I use real scaling parameter of the basis set $\chi_k(x) \rightarrow \chi_k(xe^{-\eta})$). Their analytical dependence is derived from the known behavior of the free particle confined in a large box. The new diabatic Hamiltonian is complex scaled by taking the parameter η to complex plane, $\eta \rightarrow i\theta$, which provides partial complex scaling spectrum, namely the complex resonance energy and few states of the complex rotated continuum. It is shown that the obtained complex energies correspond one-to-one with a direct application of the complex scaling method when using the same system and basis set.

In Section IV, the new method is implemented for a typi-

cal ab initio calculation of atomic resonances, which is represented by the $2s^2$ resonance of the helium atom where a large-scale basis set ExTG5G²⁸ is used. The method is fine-tuned for this purpose by adding some improvements such as a precise diabaticization method, improved analytical form for discretized continuum states due to the specific basis set, extrapolation and correction methods for the complex resonance energy. I conclude that the method is robust when using quasi-complete Gaussian basis set, yielding unique results.

In Section V, the present theoretical findings are summarized, pros and cons of the proposed method are discussed, and prospective applications are suggested.

II. THEORY

A. Methods based on a scaling of the box size

Let me start with a discussion of logical connections between the methods of complex scaling, stabilization graph, and complex absorbing potential.

First, the idea of the stabilization method is achieving a variable box size, for which different strategies are used. The most straightforward way is represented by scaling a finite basis set $\{\chi(x)\}$ directly (for a reason that will be explained later we choose the exponential form of the scaling parameter), $\{\chi(x)\} \rightarrow \{\chi(xe^{-\eta})\}$, $\eta \in \mathfrak{R}$. The box size is defined indirectly by the finite phase space, which is associated with the \mathcal{L}^2 basis set used, and effectively varied by the scaling. Adding a binding potential to the physical Hamiltonian has the same effect. For example, a binding Coulomb term was added to an electronic Hamiltonian to get stabilization graphs for molecules¹³; namely, the ionized states in the true system were replaced by the Coulomb states of the added Coulomb cone (functioning as the ‘‘box’’) and as the artificial ‘‘charge’’ was varied, the width of the Coulomb cone (the ‘‘box’’) has been effectively changed.

The real scaling of the basis set turns to complex scaling of the Hamiltonian if only the parameter η is taken imaginary. This is the basic idea of the stabilization method; an analytical continuation of energy to complex plane of η is usually done using Padé approximants. If the real potential is added, the principle of analytical continuation is applicable supposed a removal of the non-physical potential via extrapolation.

In the complex absorbing potential method, an imaginary term ($-iV(x), V(x) > 0$) is added near edges of the phase-space area covered by the basis set ($x > x_0$). This idea, based on quantum dynamics, is that the imaginary term suppresses outgoing wavefunctions; resonances, including outgoing but not incoming wave, thus become part of the \mathcal{L}^2 space. One can find here a connection to the coordinate scaling, too. Let me give an example of adding a real quadratic barrier, $V(x > x_0) = \eta^2(x - x_0)^2$. A variation of η represents a real scaling of the outer part of the basis set, namely for $x > x_0$, and would allow for a construction of a stabilization graph. The complex absorbing potential is obtained as η^2 is analytically continued to complex plane such that $\eta^2 \rightarrow -|\eta|^2 \sqrt{i}$.

B. Decoupling of a resonance and quasi-continuum at an exceptional point

Energy spectrum using any type of scalable box size allows one to distinguish between different types of energy levels which are among the states of quasi-continuum. But let me start with the bound states by pointing out that their energies are not affected by the scaling parameter, as one scales only the outer box but not the inner (e.g. nuclear) potential. The first type of the quasi-continuum states are the quasi-free states, where the particle is out of the physical potential. The quasi-free spectrum obviously depends on the box size. The second type of the quasi-continuum states are the quasi-bound states, where the particle is temporarily trapped in the physical potential, however, it might be released via the tunneling phenomenon or others. Now, the presence of the outer box creates an artificial situation where the quasi-bound particle is forced to stay bound, unless there exists a quasi-free state with a similar energy to which it can couple. Such a situation is intentionally created by varying the scaling parameter (whether η , or the charge in the case of an additional Coulomb potential, etc.). The obtained picture is of course the stabilization graph, where the spectrum is plotted in the form of potential energy curves as functions of the scaling parameter. The graph includes regions of stability, where the quasi-bound state appears as a constant energy curve, disrupted by avoided crossings as a quasi-free state approaches its energy.

Let me introduce a simple example to illustrate the ideas just mentioned – a one-dimensional model potential,

$$V = -v_0 e^{-\frac{x^2}{\sigma_0^2}} + v_1 \left[e^{-\frac{(x-x_0)^2}{\sigma_1^2}} + e^{-\frac{(x+x_0)^2}{\sigma_1^2}} \right], \quad (1)$$

where $v_0 = 7.1$ a.u., $v_1 = 4.5$ a.u., $\sigma_0 = 4$ a.u., $\sigma_1 = 2$ a.u., which supports bound states and shape-type resonances, Fig. 1. By scaling the basis set with the real scaling parameter $\exp(-\eta)$, which is here represented by the box states

$$\chi_n(x; \eta) = L_\eta^{-1/2} \sin\left(\frac{x + L_\eta}{2L_\eta} n\pi\right), \quad L_\eta = L_0 e^\eta, \quad (2)$$

one obtains the stabilization graph shown in Fig. 2.

Formally, the complex scaling method corresponds to taking an imaginary value of the scaling parameter η . It is thus basic to understand what happens to the spectrum as η is taken to the complex plane. It is known since the stabilization method has been proposed that each avoided crossing on the real axis is associated with an exceptional (branching) point singularity (EP) in the complex plane, see Ref.¹¹. Two selected avoided crossings and EPs are demonstrated for our model in Fig. 3. EPs often indicate a boundary between different qualitative modes of the system studied^{29–31}. The present case is no different. Before reaching an EP, we find avoided crossings created due to mixing of two adiabatic states, but after the EP there are two diabatic-like states crossing each other, where one is clearly the resonance while the other is a detached quasi-bound state. Apparently, the EP is associated

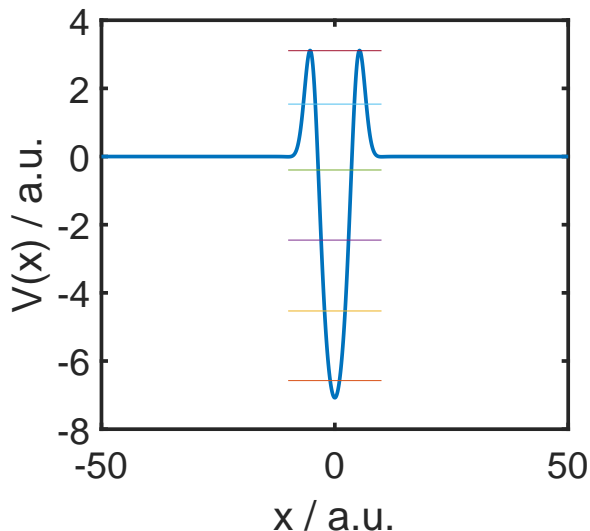


FIG. 1. Model one-dimensional potential, Eq. 1, used for present demonstrations, supports bound states and resonances shown by the energy levels.

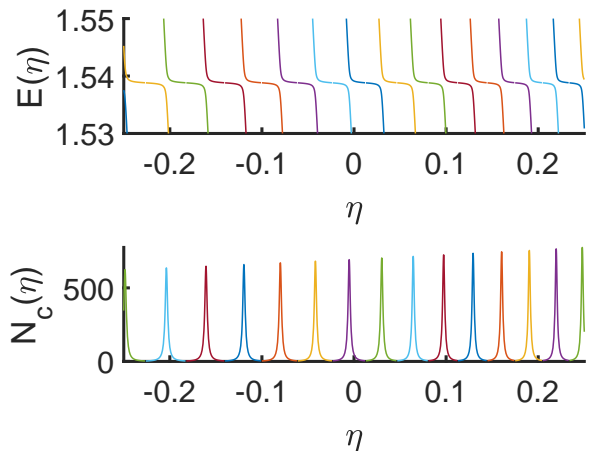


FIG. 2. (a) Stabilization graph near the energy of the first resonance $E_r = 1.5388$ a.u.. These results are based on the box size of $L_0 = 50$ a.u. and the number of basis functions $\max(n) = 500$, Eq. 2. (b) Non-adiabatic coupling elements $\langle \psi_1 | d/d\eta | \psi_2 \rangle$ corresponding to the avoided crossings. $N_c(\eta)$ are later used in a diabaticization procedure to construct 2×2 diabatic Hamiltonians corresponding to the avoided crossings.

with a *adiabatic to diabatic spectral transition*, which takes place in the complex plane of the scaling parameter η .

III. COMPLEX SCALING APPLIED EX POST TO HERMITIAN SPECTRUM

A. Basic assumptions

In the second part of the article I will show how all this can be used to calculate the complex resonance energy. The method starts from the stabilization diagram. First note that

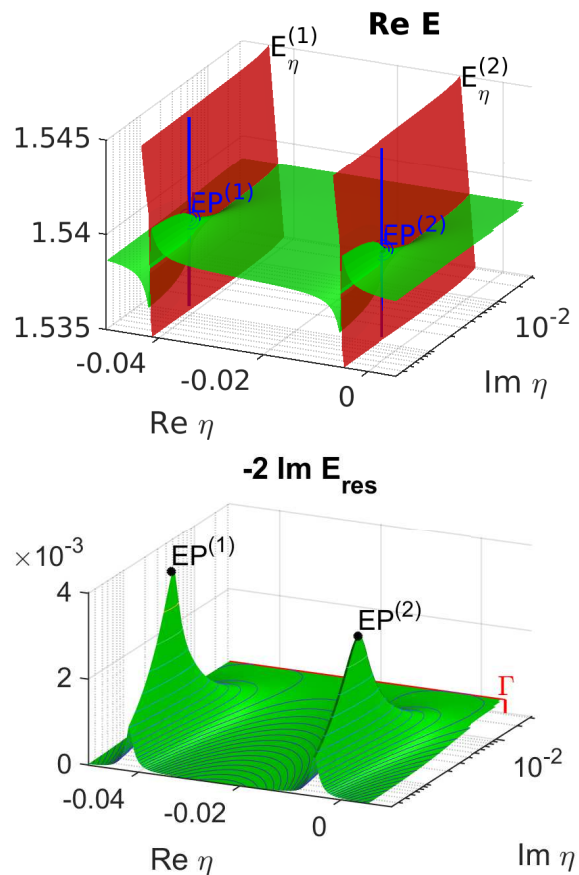


FIG. 3. Illustration of the analytical continuation of the real scaling parameter to the complex plane. As an imaginary part is added to the scaling parameter η , the energy splitting at the avoided crossings becomes smaller. This trend continues until the corresponding exceptional points ($EP^{(1)}$, $EP^{(2)}$) are reached. Beyond the EPs, the avoided crossings are no more present, instead, the real parts of the energy surfaces for the resonance and quasi-continuum cross each other. This phenomenon can be interpreted as a natural diabaticization at the exceptional point. The imaginary part of resonance energy E_r is stabilized far in the complex plane of η (note the logarithmic scaling of $\text{Im } \eta$), where it corresponds to the physical resonance width Γ .

the avoided crossings are relatively far apart, so that in a good approximation a contribution of only two states can be assumed.

Another important observation is that the EPs are located relatively near the real axis (the value of $\text{Im } \eta$ to find the EP is in fact an order of magnitude smaller than values of the same quantity where the resonance width has converged to Γ (see Fig. 3b)). Thus the first premise of the new method is that the avoided crossing of the real energies belongs to the immediate vicinity of the near EP; the EP determines the parameters of the avoided crossing and vice versa these parameters can be used to determine the EP.

As discussed above, the complex resonance energy is found on the opposite side of the EP. Not only that, but even at a relatively large distance from it (see Fig. 3b). Two things are learnt from this circumstance. First, it is necessary to cor-

rectly design the dependence of the quasi-continuum energy on the scaling parameter η . For example, if a linear dependence was used as the simplest option, a linear decrease of the resonance width instead of its stabilization with $\text{Im}\eta$ would be the wrong result. Second, the area where the complex resonance energy is stabilized is so distant that the widths of the continuum states far exceed the separations of the EPs; thus the area belongs to the common neighborhood and influence of a number of EPs.

B. From avoided crossings to EPs

Avoided crossings are found in the stabilization diagram for certain real values of $\eta = \{\eta_{c1}, \eta_{c2}, \dots\}$. Clearly, a diabatic crossing (when no coupling is present) would occur exactly at the point where the energies of the resonance E_r and the box state E_η are equal. A diabatic Hamiltonian near the avoided crossing reads such as

$$H = \begin{bmatrix} E_r & \delta/2 \\ \delta/2 & E_\eta \end{bmatrix}. \quad (3)$$

By using a standard diabaticization procedure, it is easy to fit a particular problem to this formula, where it is found that E_η dependence on η is nearly linear:

$$E_\eta = E_r - a \cdot (\eta - \eta_c), \quad (4)$$

whereas the other parameters E_r and δ are more or less constant within the range of the crossing. The solutions of the diabatic Hamiltonian, Eq. 3, are given by

$$\varepsilon_\pm = E_r + \frac{E_\eta - E_r}{2} \left[1 \pm \sqrt{1 + \left(\frac{\delta}{E_\eta - E_r} \right)^2} \right]. \quad (5)$$

Clearly, the potential curves are at the closest attachment on the real axis for $E_\eta = E_r$, where

$$(\varepsilon_+ - \varepsilon_-)|_{\eta=\eta_c} = \delta. \quad (6)$$

The exceptional point occurs for complex $\eta = \eta_{EP}$, where

$$E_\eta - E_r = -i\delta, \quad (7)$$

from where the degenerate complex energy is given by

$$\varepsilon_\pm|_{\eta=\eta_{EP}} = E_r - \frac{i\delta}{2}. \quad (8)$$

C. Dependence of quasi-continuum on the axis scaling parameter η

As long as the box is small, we find out distinct avoided crossings in the stabilization graph, where the resonance state is represented by a nearly constant (real defined) energy E_r . On

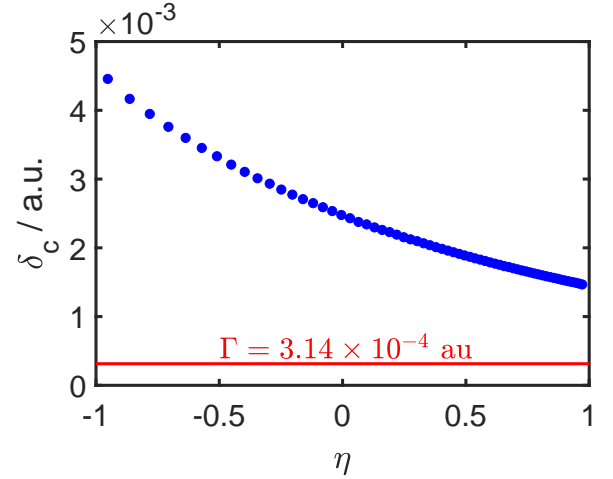


FIG. 4. Energy splittings δ_c for the avoided crossings defined by their positions $\eta = \eta_c$ in the stabilization graph. The energy splittings converge to the resonance energy width $\Gamma = 3.14 \times 10^{-4}$ a.u. in the limit $\eta \rightarrow \infty$.

the other hand, the intersecting curve of E_η , which is decreasing with η , represents a particle freely moving outside of the potential, within the box. We find the dependence on η using the Schrödinger free particle equation:

$$-\frac{\hbar^2}{2\mu} \frac{\partial^2}{\partial x^2} \psi(x) = E_0 \psi(x), \quad (9)$$

where upon the scaling the wavefunction is changed such as $\psi(x) \rightarrow \psi(xe^\eta)$. Expectably, this would also bring about the energy change, $E \rightarrow E_\eta$:

$$-\frac{\hbar^2}{2\mu} \frac{\partial^2}{\partial x^2} \psi(xe^\eta) = E_\eta \psi(xe^\eta). \quad (10)$$

By changing the variable $x' = xe^\eta$ we get:

$$-\frac{\hbar^2}{2\mu} \frac{\partial^2}{\partial x'^2} \psi(x') = e^{2\eta} E_\eta \psi(x'). \quad (11)$$

By comparing Eqs. 9 and 11 we get the dependence of the free particle states upon the scaling parameter,

$$E_\eta = E_0 e^{-2\eta}. \quad (12)$$

To match the dependence of Eq. 4 with that of Eq. 12 as close as possible, I make use of the approximation

$$E_\eta = E_r \left[1 - \frac{a}{E_r} (\eta - \eta_c) \right] \approx E_r e^{-\frac{a}{E_r} (\eta - \eta_c)}. \quad (13)$$

As one would find empirically, the exponent a/E_r is not given exactly by 2, see Fig. 5, calling into question the validity of Eq. 12. This discrepancy is perhaps explained by the influence of non-zero potential even if the particle is moving outside of the potential trap, which is the case especially if the box is small (small values of η_c).

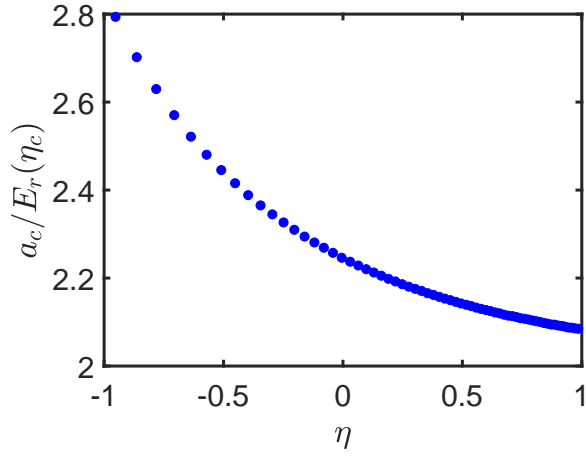


FIG. 5. Resonance and quasi-continuum states are diabatically at the avoided crossings, such that they cross for η_c . The diabatic quasi-continuum energy E_η is given by a linear curve in η with the slope of a_c in the short interval of the avoided crossing. However, the long range behavior of the quasi-continuum energy is exponential such that $E_\eta \propto \exp(-2\eta)$, which applies in the limit of the infinite box size. This plot shows that the actual exponent at the avoided crossings is larger than the limiting value of 2, $E_\eta \propto \exp[-a_c/E_r(\eta_c) \cdot (\eta - \eta_c)]$.

D. Cooperate remote behavior of exceptional points

As discussed earlier, the EPs are located near the real axis of the scaling parameter η and thus they can be determined by using the avoided crossings in the stabilization graph. To find the complex resonance energies, however, it is necessary to explore the behavior of the complex energies beyond the EPs, far in the complex plane of the scaling parameter η .

Let me remind now that some stabilization methods rely on a very precise and fine fitting of the region near a single EP to get a good approximation for the distant regions where the resonance energy gets stabilized¹¹. Some other works rely on a fine fitting of the region between the avoided crossings. As one can see in Fig. 3 that both approaches are justified due to the principle of analytical continuation.

Here we introduce a different approach. While it is based on a physically justified dependence for the diabatic states near avoided crossings, Eq. 13, the analytical form is too simple to suffice for an application of the analytical continuation principle.

Clearly, as η is taken into complex plane, the width of the quasi-continuum states is increased, Eq. 13. One can view these states (taken to the complex plane), as a number of energy intervals which overlap. In this picture, many quasi-continuum states overlap near the resonance energy E_r , and therefore are bound to have some contributions to the resonance. In order to take into account more states of the quasi-continuum, it is possible to construct the diabatic Hamiltonian

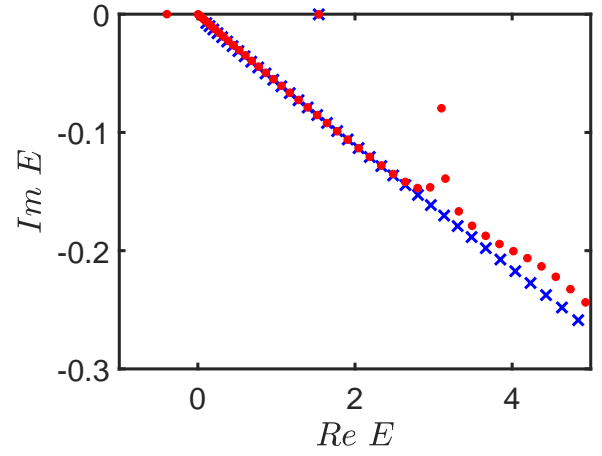


FIG. 6. This is the spectrum of the Hamiltonian constructed from several avoided crossings on the stabilization graph ('x'), where the complex scaling was applied ex post to the quasi-continuum states, see Hamiltonian in Eq. 14, $\eta = 0.025i$. It is compared with the calculation where the complex scaling was applied directly to the x -axis in the Hamiltonian ('•'). The same basis sets were used for both calculations.

for several avoided crossings as a single matrix

$$H(\eta) = \begin{bmatrix} E_r(\text{Re}\eta) & \delta_{c1}/2 & \dots & \delta_{c,n}/2 \\ \delta_{c1}/2 & E_{r1} e^{-\alpha_1(\eta-\eta_{c1})} & \dots & \\ \dots & \dots & \dots & \\ \delta_{c,n}/2 & & & E_{r,n} e^{-\alpha_n(\eta-\eta_{c,n})} \end{bmatrix}, \quad (14)$$

where α_j are defined as

$$\alpha_j = \frac{a_{c,j}}{E_{r,j}}. \quad (15)$$

This Hamiltonian is based on the 2×2 diabatic Hamiltonians for the individual avoided crossings on the real axis (Eqs. 3 and 13). The spectrum of the Hamiltonian $H(\eta)$ corresponds to that of the usual complex scaled Hamiltonian, see Fig. 6. The difference is that now only one resonance is obtained in the non-Hermitian spectrum. This method can be understood as a *complex scaling applied onto the real spectrum, i.e. ex post* the Hermitian calculation.

A sufficient number of the quasi-continuum states must be included in Eq. 14 to accurately reproduce the resonance energy. The plots in Fig. 7 show how the resonance energy is changed as the quasi-continuum states are added one by one starting from the avoided crossing for the smallest size of the box $L \approx 20$ a.u. up to the largest box of $L \approx 130$ a.u., which correspond to the interval of the scaling parameter $-1 < \eta_c < 1$.

The most significant change of the result occurs when the states participating on the avoided crossings for the box size of $L \approx 50$ a.u. are included, Fig. 7. This value corresponds to the box size when no scaling is used, $\eta = 0$. These particular states participate on the EPs which are the nearest to

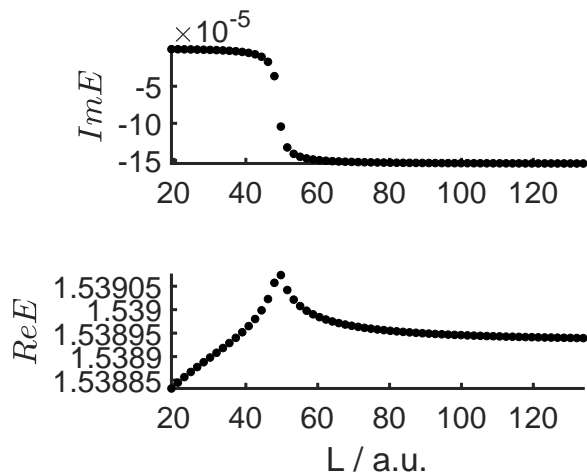


FIG. 7. Dependence of the resonance energy on the size of the Hamiltonian (Eq. 14, $\eta = 0.01i$), as the contributions of subsequent EPs (which correspond to the avoided crossings in the stabilization graph) are added. The horizontal axis shows the box size at which the EP, which was added, is found. So the first point has been obtained for a 2×2 Hamiltonian using one EP ($L_c = 19.3$ a.u.), the second for a 3×3 Hamiltonian using 2 EPs ($L_{c1} = 19.3$ a.u., $L_{c2} = 21.1$ a.u.), etc..

the calculated point in the complex plane, which is defined by $\eta = 0.01i$.

A stabilization of the resonance energy with the increasing complex scaling parameter $\theta \equiv -i\eta$ is demonstrated in Fig. 8, where it is compared with the result of the usual complex scaling method for the same box size ($L = 50$ a.u.) and basis set ($N = 500$).

Notably, the error of the resonance width (imaginary value of its complex energy) linearly increases with θ where it should be stabilized according to the benchmark calculation. This is a convergence problem, where for larger values of θ , a larger size of the diabatic Hamiltonian is required, namely it is necessary to include more avoided crossings corresponding to large values of η_c .

The real part of the resonance energy is stabilized for large values of θ , however it includes a constant error. This error is decreased as more quasi-continuum states are added for the large box sizes. This indicates that also this error is a matter of convergence.

Should a full convergence be obtained, the avoided crossings for large boxes are necessary. This in turn requires using more basis functions for the Hermitian calculations. Using extrapolation to obtain parameters for the distant avoided crossings ($\eta_c \gg 1$) may help to meet this requirement in practical applications to quantum chemistry.

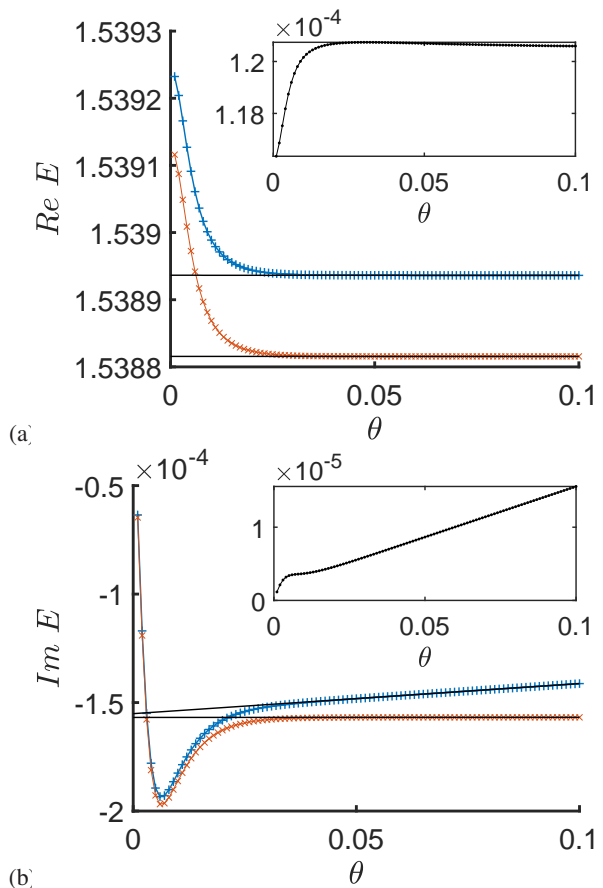


FIG. 8. Complex resonance energy which has been obtained using the diabatic Hamiltonian (Eq. 14) constructed from several EPs corresponding to the avoided crossings in the stabilization graph for $-1 < \eta_c < 1$. The diabatic Hamiltonian has been complex scaled by using $\eta = i\theta$, (blue '+'). As a benchmark, the result from the usual complex scaling method is plotted (red 'x'). The insets show the difference between the approximate and benchmark calculations.

IV. APPLICATION FOR HELIUM DOUBLY EXCITED STATES

A. Summary of the new methodology

Let me demonstrate how the described findings can be used as a method for calculation of atomic resonances.

The proposed method is based on using a large scaling interval. It is therefore necessary to choose a basis set which enables this without a significant precision loss. Here I show full-CI calculation of doubly excited $2s^2$ state of helium using exponentially tempered primitive Gaussian basis sets ExTG5S and ExTG5P optimized for up to four excited bound states at seven digits of accuracy²⁸.

In the case of one-dimensional model a standard diabaticization procedure, based on integrating over the non-adiabatic coupling element, has been used. Its application to atomic calculations would be cumbersome. Below I propose a suitable diabaticization procedure which avoids calculations of non-adiabatic coupling elements, being based solely on a precise

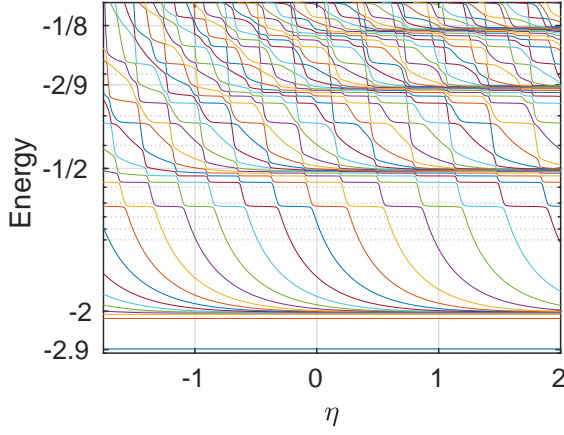


FIG. 9. A stabilization graph obtained for helium via real scaled Gaussian basis set in the s -limit. All states up to the two-electron ionization limit, $E = 0$, are plotted, where the energy is shown in the logarithmic scale to comprehend all available one-electron ionization thresholds at $-2 E_h$, $-1/2 E_h$, etc.. The ground state level is shown at $-2.9 E_h$. Resonances are manifested by constant energy curves which are disrupted with various avoided crossings with the continuum states. The discretized continuum states are characterized via exponential decay of their energy with the real scaling parameter η , where they converge to the limits associated with the corresponding ionization thresholds.

fitting the potential energy curves.

I improve the procedure in several other aspects such as: (i) I suggest to find a correct analytical fit for the quasi-continuum by including parts of the potential energy curves of decoupled quasi-continuum states. (ii) As in the case of the one-dimensional model potential, also in atomic application, the complex resonance energy for large values of θ sort of drifts out of the correct value, which requires a backward extrapolation to $\theta \rightarrow 0$. (iii) It is found that the real part of complex resonance energy is quite underestimated where the error corresponds to the shift of the ionization potential due to the finite size of the basis set.

B. Diabatization procedure using *ab initio* energies

Let us start our discussion with the s -limit, which means that the atomic basis set is represented only by the s -type functions. The corresponding calculations are very fast and allow us to calculate a large scale stabilization graph, which is shown and described in Fig. 9.

The next goal is to construct the diabatic Hamiltonian defined in Eq. 14 for a selected helium resonance. We will study the resonance $2s^2$, which is the lowest metastable state above the first ionization threshold near the energy $-0.8 E_h$, see Fig. 9. The real Hermitian calculations led to thirteen avoided crossings with different quasi-continuum states as the real scaling parameter η varied in the interval $-1.75 \leq \eta \leq 2$.

As the first step we determine two-by-two diabatic Hamiltonians (Eq. 3) corresponding with the individual avoided crossings. Let us present here a summary of a robust algo-

rithm suitable for this task.

At first we select points in the potential energy curves defined by a confined energy interval near the resonance energy. In our case, we used the interval of $\pm 0.1 E_h$ around the resonance energy $-0.723 E_h$, which we could estimate from the stable parts of the stabilization graph, Fig. 9. This step allows us split individual avoided crossings which are processed individually in the next steps.

Real resonance energy E_r and coupling element δ are obtained in two steps of the predictor-corrector type.

1. Predictor

For each avoided crossing we calculate a first estimate of δ and E_r which define the diabatic Hamiltonian Eq. 3. For this sake we use definition of δ as the minimum energy split, Eq. 6. In practice we use spline interpolation for the split $(\epsilon_+ - \epsilon_-)$ on the axis of η between the known *ab initio* points, and find δ as the interpolated minimum at $\eta = \eta_c$.

Based on Eq. 5 we get the relation between the sums of adiabatic and diabatic energies,

$$\epsilon_+ + \epsilon_- = E_r + E_\eta. \quad (16)$$

We use the fact that the diabatic energies E_r and E_η are equal at the point $\eta = \eta_c$, i.e.,

$$E_r = \frac{\epsilon_+ + \epsilon_-}{2} \Big|_{\eta=\eta_c}, \quad (17)$$

to get E_r . Namely, we calculate the mean adiabatic energy $(\epsilon_+ + \epsilon_-)/2$ for the *ab initio* points within the avoided crossing interval, and then we use the spline interpolant to get the estimate of E_r at the point η_c obtained before.

As a matter of fact, the algorithm described here as *predictor* is not robust, as the precision of η_c largely relies on the spline interpolation. Yet the above obtained parameters δ and E_r provide a well needed estimate for the precision procedure described as *corrector*.

2. Corrector

We determine the values of E_r and δ in a robust way by fitting them to all *ab initio* points within the avoided crossing. We use the fact that E_r and δ must represent constants along the examined interval of η . δ and E_r are expressed using the adiabatic energies such that,

$$\begin{aligned} \delta &= \sqrt{\Delta_\epsilon^2 - 4(\bar{\epsilon} - E_r)^2}, \\ E_r &= \text{sign}(E_r - \bar{\epsilon}) \cdot \frac{\sqrt{\Delta_\epsilon^2 - \delta^2}}{2} + \bar{\epsilon}, \end{aligned} \quad (18)$$

where we define

$$\bar{\epsilon} = \frac{\epsilon_+ + \epsilon_-}{2}, \quad \Delta_\epsilon = \epsilon_+ - \epsilon_-. \quad (19)$$

We substitute $\Delta_\varepsilon(\eta_k)$ and $\bar{\varepsilon}(\eta_k)$ for each *ab initio* point η_k within the avoided crossing. Using the estimated values of E_r and δ on the right hand sides of the equations we obtain the values $\delta(\eta_k)$, $E_r(\eta_k)$. These values should be η independent supposed that the values for δ and E_r on the right hand side were correct. In reality, they are not, which may be used to get the right values by imposing the requirement of constancy in a minimization procedure. We define a quantity σ based on the standard deviation from the mean values of $\delta(\eta_k)$, $E_r(\eta_k)$ such that,

$$\begin{aligned}\sigma &= \sqrt{\sigma_1^2 + \sigma_2^2}, \\ \sigma_1^2 &= \frac{1}{N} \sum_k \left[E_r(\eta_k) - \frac{\sum_k E_r(\eta_k)}{N} \right]^2, \\ \sigma_2^2 &= \frac{1}{N} \sum_k \left[\delta(\eta_k) - \frac{\sum_k \delta(\eta_k)}{N} \right]^2.\end{aligned}\quad (20)$$

Then we find parameters δ and E_r associated with the minimum value of σ using a standard minimization procedure. The algorithm described as *predictor* is useful for getting an initial estimate for the numerical calculation.

3. Improving *ab initio* data

Parameter δ (and also η_c , see below) should form a regular series as obtained for the set of neighboring avoided crossings. If this is not the case, calculations must be improved by adding *ab initio* data. In practice, we take the calculated new values of η_c (see below) for which we run additional *ab initio* calculations. After repeating the whole procedure three to four times, well converged parameters (E_r , δ , and η_c) are finally obtained.

C. Fitting form for quasi-discrete continuum

Finally, we need to determine the parameters which characterize the diabaticized quasi-continuum state, α_c and E_0 , as involved in each avoided crossing.

Let us propose a new form for the continuum states given by

$$\begin{aligned}E_{\eta,k} &= (E_r - E_0) e^{-\alpha_{c,k}(\eta - \eta_{c,k}) - \beta_{c,k}(\eta - \eta_{c,k})^2} \\ &+ E_0,\end{aligned}\quad (21)$$

which differs from Eq. 13, which was suggested above for the one-dimensional testing case, in the following aspects.

First, Eq. 21 reflects the fact that the first ionization continuum is not zero but it is given by the energy of ground state He^+ ion, $E_0 = -2 E_h$. In fact, due to the variational principle, the energy of the helium ion for the particular basis set should exceed the infinite basis set limit of $-2 E_h$. In the case of a Gaussian finite basis set, apparently, the quasi-continuum state always ends up below the threshold as it is

transformed into a highly excited Rydberg state for $\eta \rightarrow \infty$, see Fig. 9. Here, for simplicity, we will use the true limiting value, $E_0 = -2 E_h$, in Eq. 21. Within the fitting procedure used for the quasi-continuum, which will be described below, there will be a need to exclude the area where the quasi-continuum state has changed to the Rydberg state.

The second aspect where Eq. 21 has been modified from Eq. 13, is represented by the quadratic dependence of the exponent on η . In Section III C we derived the exponential dependence for the case of a finite box supposed that the discrete basis set is infinitely large, where we found also the value of the linear coefficient, $\alpha_c = 2$. It was found empirically that when the box size is finite, α_c deviates from 2, see Fig. 5. Additionally, the Gaussian basis set used for the present case fills the phase space in a subtle way which differs from the box basis sets. The *ab initio* data displayed in Fig. 9 confirm the general exponential dependence of the energy of the quasi-continuum, see the curves between the first ionization threshold ($-2 E_h$) and the first resonance ($-0.72 E_h$). Yet, these curves cannot be fitted precisely enough to a linear exponential, therefore a quadratic polynomial has been introduced empirically for the exponent.

1. Using quasi-discrete continuum outside and within avoided crossings

To obtain the best fit of quasi-continuum, we need a large portion of the curve defined by *ab initio* data. The *ab initio* curve constitutes from the *isolated quasi-continuum* (see Fig. 9 in the interval $-1.75 E_h > E_\eta > -0.8 E_h$). Note that we excluded energies below $-1.75 E_h$. The reason is that the quasi-continuum states change to Rydberg states as their energies drop down near the threshold energy.

The next part of the quasi-continuum curve, beyond $E_\eta = 0.8 E_h$, is *embedded in the avoided crossing*. In the area of avoided crossing, E_η can be determined based on the mean value of the crossing curves, using the known value for E_r , as given in Eq. 16.

2. Fitting procedure for quasi-discrete continuum

We start by determining the parameter η_c in Eq. 21, for which we use only the part of the quasi-continuum curve which was originally embedded in the avoided crossing. We use a simple parabolic fit for $E_\eta(\eta_k)$ such that

$$E_\eta(\eta_c) \approx a_2 \eta^2 + a_1 \eta + a_0, \quad (22)$$

from which we determine the value of η_c such that

$$E_\eta(\eta_c) = E_r. \quad (23)$$

The next step is to determine α_c and β_c in Eq. 21, for which we use the full quasi-continuum curve composed of the isolated and embedded parts as discussed above. We apply the

weighted least square fitting of

$$f_i \equiv \log \frac{E_\eta(\eta_i) - E_0}{E_r - E_0} \quad (24)$$

to the second order polynomial

$$f_i \approx -\alpha_c(\eta_i - \eta_c) - \beta_c(\eta_i - \eta_c)^2, \quad (25)$$

where the weights are given by,

$$w_i = \frac{E_r - E_0}{E_\eta(\eta_i) - E_0}. \quad (26)$$

D. Complex scaling – stabilization for $\theta \gg 0$ and backward extrapolation to $\theta \rightarrow 0$

At this point we have all parameters needed to construct the Hamiltonian according to Eq. 14, having in mind the modification concerning the η -dependence of the quasi-continuum, Eq. 21. The complex scaled Hamiltonian is obtained by setting

$$\eta = i\theta + \Delta_\eta, \quad 0 < \theta < \frac{\pi}{4}. \quad (27)$$

Δ_η is a small real parameter which will allow us to see the dependence of results on a real scaling of the basis set. By diagonalizing the complex scaled Hamiltonian, we obtain the typical picture including the rotated quasi-discrete continuum, and the resonance. Let us discuss the dependence of the obtained complex resonance energy on the complex scaling parameter θ , which is displayed in Fig. 10.

The complex energies demonstrate high instability for $\theta < 0.4$, where they largely depend on Δ_η . This is due to the fact that Δ_η effectively changes the position with respect to the branch points along the real axis in Fig. 3.

According to the theory in Section III, which was also approved by the one-dimensional numerical experiment, the complex resonance energy should be constant as θ is large enough. In fact, the one-dimensional calculation shows that the imaginary part of the resonance energy is mildly linearly dependent on θ in the stable part of the complex plane, however the first derivative of this dependence can be pushed down to zero when increasing the basis set.

Here, Fig. 10, the stable part is characteristically almost independent on the real scaling shift Δ_η . However, the complex energy, both real and imaginary components of it, show a low order polynomial dependence on θ . We explain this artifact as a result of the finite size of the basis set. Namely, the only states which depend on the scaling η in the diabatic Hamiltonian, are represented by the quasi-continuum, but we could see above that the quasi-discrete continuum has a specific dependence on η which is different from the finite basis set, see Eq. 21.

In other words, the finite Gaussian basis set, optimized for calculations of the atomic states as is, deteriorates by the application of real scaling which apparently brings in a systematic error as the scaling parameter is analytically continued to

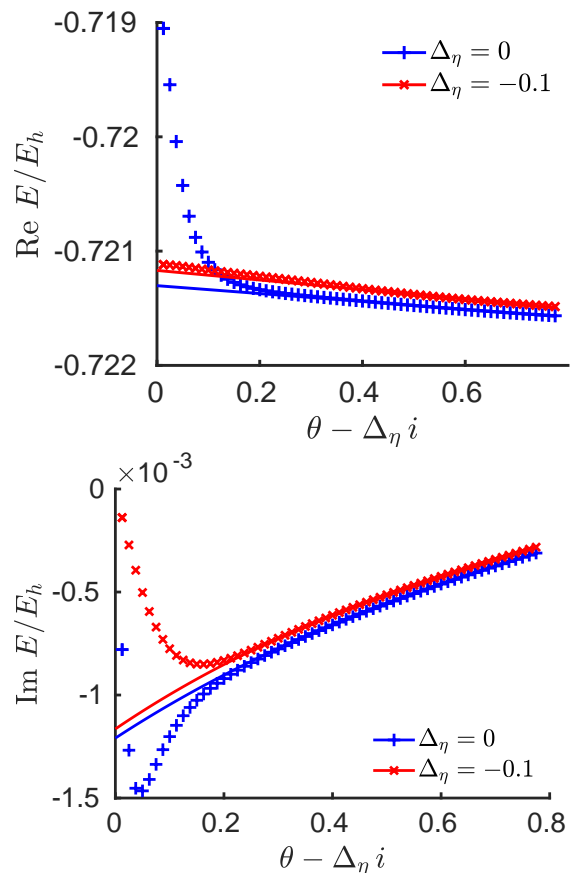


FIG. 10. Complex resonance energy of the helium $2s^2$ state based on the Hermitian calculation of the stabilization graph (Fig. 9). The stabilization graph allows us to determine the dependence of energies on the real parameter η , which scales the basis set, in the form of a diabatic Hamiltonian which includes several quasi-continuum states and the resonance (Eq. 14). By bringing the real scaling to the complex plane, $\eta \rightarrow i\theta + \Delta_\eta$, we obtain the complex scaled Hamiltonian which is diagonalized and the complex resonance energy is obtained (markers +, ×). The real and imaginary parts of the resonance energy are greatly unstable for $\theta < 0.4$, as they pass near branch points, compare Fig. 3. The stable part for $\theta > 0.4$ is characterized by a low order polynomial dependence on θ , which can be used to a backward extrapolation to $\theta = 0$ as shown by the lines. The disturbing fact that the resonance energy is not constant even for large values of the complex scaling parameter θ is probably explained by the finite size of the basis set, see the text.

the complex plane. This error must be removed by an extrapolation from the stable region $\theta > 0.4$ as if back to $\theta = 0$ as shown by the solid lined in Fig. 10.

The complex resonance energy which is obtained for $\Delta_\eta = 0$ is given by $E_{2s^2} = (-0.7213 - 1.2 \times 10^{-3}i) E_h$. The value which is obtained via direct application of the complex scaling with the same basis set is given by $E_{2s^2} = (-0.7228358 - 1.199 \times 10^{-3}i) E_h$, which also represents the true s -limit for this state, see Ref.³² and references therein. Clearly, the real scaling method provides a correct result yet with much larger error bars compared to a direct application of complex scaling when using the same high quality Gaussian basis set.

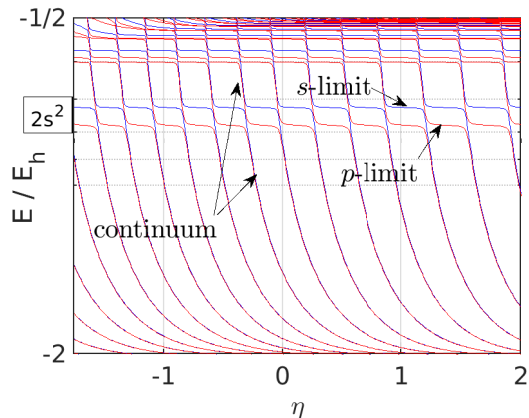


FIG. 11. Effect of increasing of the rotational basis set – comparison of stabilization graphs in the s and p -limits. The energy of the $2s^2$ resonance is decreased upon adding the p symmetry, while the energy split of the avoided crossings is increased about twice. On the other hand, the quasi-continuum states are almost intact by adding the p symmetry, as they correspond to the He^+ $1s$ state which has the pure s symmetry.

E. Method to increase rotational basis set

Up to now we used only the s -type Gaussians to calculate the $2s^2$ doubly excited resonance of the helium atom. It is known however that including also the p -type functions leads to a significant increase of the resonance width, see Ref.³² and a notable decrease of the resonance energy. This is in harmony with the present findings demonstrated in the comparison of the stabilization graphs for the s and p -limits, Fig. 11. While the decrease of the real part of the resonance energy with including the p symmetry is obvious, in particular the increase of the resonance width can be anticipated from the larger split of the avoided crossings.

Calculation of massive data when including the p symmetry is still computationally feasible and fast, at least in this system. However, as the rotational basis set is more increased, the calculations become costly. Therefore we propose using the following computational strategy. The positions η_c calculated for the s limit serve as the initial guess for the higher p limit, where we calculate small sets of ab initio points near every avoided crossing. Then we use again the predictor-corrector method described in Section IV B to calculate δ^p , E_r^p , and η_c^p , now in the precision of the p -limit. After the parameters in the p -limit are known, we proceed in the same manner to the d -limit to get δ^d , E_r^d , and η_c^d , and the same could be done also even for higher rotational numbers.

To construct the Hamiltonian Eq. 14, we need to include the diagonal terms for the continuum states as well. We proceed according to Section IV C, where the continuum is fitted to Eq. 21 using two parts of the quasi-continuum curve – isolated quasi-continuum, and quasi-continuum embedded in the avoided crossing. Now, we use the fact that the isolated part of the quasi-continuum curve is intact by adding the higher rotational symmetries, see Fig. 11, thus the ab initio data obtained

for the s -limit can be used for this part.

We calculated the complex resonance energy p -limit using the above indicated algorithm and algorithms discussed for the s -limit. The results are shown in Fig. 12. The calculations were repeated for an interval of the real basis set scaling $\Delta\eta$, Fig. 12, showing a mild dependence on this parameter. The obtained resonance energy is given by $-0.775 - 2.37 \times 10^{-3}i E_h$, which must be compared with the benchmark value $-0.777296 - 2.332 \times 10^{-3}i E_h$ obtained for the same basis set when the Hamiltonian is complex scaled directly, Ref.³².

The error of the present calculation is given by $+0.002 - 0.00004i E_h$, which shows that the error of the real part is two orders of magnitude larger then the error of the imaginary part. Note that the same discrepancy occurs for the complex resonance energy in the s -limit above. Interestingly, the real shift of the resonance energy is comparable with the energy depth (below the ionization threshold) of the last Rydberg state which can be obtained within the used basis set. If the energy depth of the last Rydberg state is subtracted from the real part of the resonance energy, we obtain the “corrected” resonance energy $-0.77728 - 2.37 \times 10^{-3}i$ where the error of the resonance position is given by $0.00002 E_h$, now comparable with the precision of the width. The corrections differ for different values of $\Delta\eta$, Fig. 12, corresponding to the last Rydberg state within the real scaled basis set defined by the scaling parameter $\eta = \Delta\eta$.

V. CONCLUSIONS

Hermitian (stabilization) methods for calculations of resonances all boil down to manipulations with the box size controlled by a “scaling” parameter η . The result is represented by the stabilization graph, which includes the energy spectrum as dependent on the scaling parameter η . The potential energy curves near an energy of a quasi-bound state include intervals of η where the energy is stable. The intervals of stability are interrupted with avoided crossings due to an interaction with the quasi-free states of the “box”. Each of the avoided crossings corresponds to an exceptional point (EP) in the complex plane of the box scaling parameter η .

I suggest that the EPs can be interpreted as marking a transition between two qualitatively different descriptions of the problem, where on one side the resonance and the quasi-continuum are coupled (which is reflected in the presence of the avoided crossings), while on the other side of the EP, the resonance state is decoupled from the quasi-continuum (the potential energy curves of the resonance and quasi-continuum cross each other).

I suggest a new method to calculate the complex resonance energy from the stabilization graph. Its main idea is represented by appreciating the fact that the resonance energy is stabilized *deep* in the complex plane of η where energies of *quasi-continuum states* are characterized by *large imaginary parts*, in other words, the quasi-continuum states have large energy widths and therefore *many* such states *overlap near the position of the resonance*. Therefore *all* these states must be included in a diabatic basis set for the resonance.

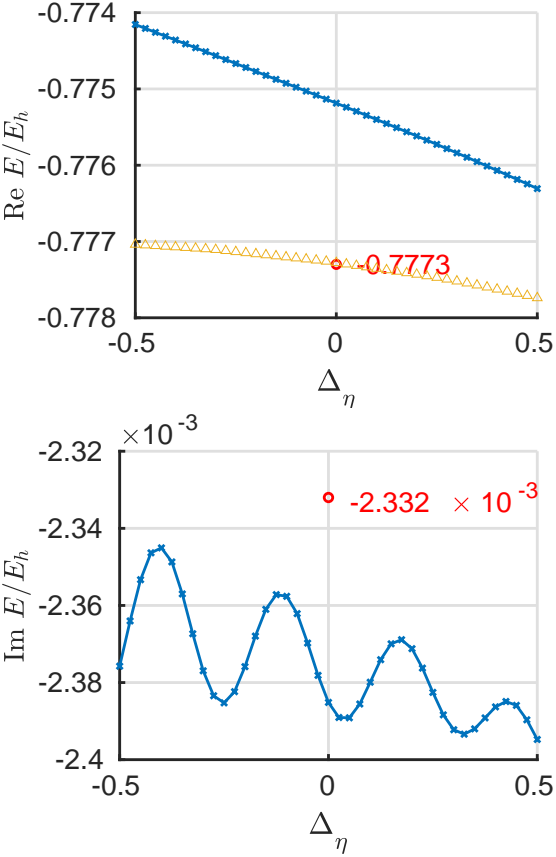


FIG. 12. Complex energies of the $2s^2$ helium resonance obtained for the p -limit using real scaled basis set calculations are displayed. Cross markers show the results which are obtained as indicated in Fig. 10, i.e. via extrapolation to $\theta \rightarrow 0$. The results depend on the real scaling shift Δ_η , where the optimal basis set is represented by $\Delta_\eta = 0$ (namely, this point represents the original unscaled basis set). The circle markers display the results obtained using the same basis set when complex scaling is applied to the electronic Hamiltonian; they also represent the benchmark values, Ref.³². The triangles for the real part of the complex resonance energy represent a “corrected” result, which is obtained by adding the energy difference between the true ionization potential and the energy of the last bound state within the final basis set.

In accord with this I proposed a diabatic Hamiltonian which is constructed using multiple avoided crossings, where each crossing brings in another quasi-continuum state. The diabatic Hamiltonian, which is constructed, is parametrized by the real scaling parameter η . The diabatic Hamiltonian is then analytically continued to the complex plane through $\eta \rightarrow i\theta + \Delta_\eta$. Diagonalization of such a Hamiltonian leads to the complex energy spectrum which includes both the resonance and the rotated quasi-continuum; it is in fact directly comparable with the result obtained via the usual complex scaling method with the same basis set.

The new method is developed using a one-dimensional model potential where a semi-complete basis set is used. Then the same method is adapted to calculate complex scaled spectrum of the helium atom, where again a large scale basis set is

used. Let me summarize the pros and cons of the new method.

(i) In contrast to other similar methods based on stabilization graph, this method does not provide a single resonance energy, rather it provides a whole *part of the complex scaled spectrum* including the resonance *plus* several quasi-continuum states. As such it lends itself directly for calculations of photoionization resonances (and cross-sections) via methods such as (t, t') ^{25–27} where inclusion of quasi-continuum states is unavoidable.

As another advantage of handling with a portion of the spectrum, it is well thinkable to extend the diabatic Hamiltonian to include even several resonances and bound states. Such extension would allow to calculate complex transition dipole moments between resonances and bound states which are experimentally measurable via absorption Fano profiles³³. The transition dipole moments between bound and resonance states also play a major role in a realization of a recently described phenomenon of Rabi-to-RAP (Rapid Adiabatic Passage) transition within dynamical encircling of exceptional point in the frequency-laser amplitude plane^{34,35}.

(ii) Interestingly, the application of complex scaling on the diabatic Hamiltonian which was obtained via fitting on the real scaled basis set does not inherit numerical problems which are typical for large values of complex scaling parameter θ when the system Hamiltonian is complex scaled directly. Such errors were observed in corresponding complex scaling calculations of helium atom (Ref.³², Fig. 4) and were explained in a general detailed study of the complex scaling method¹. Here within the present method, a stable complex spectrum is obtained even up to the limit $\theta \rightarrow \pi/4$ (Fig. 10).

(iii) The present method requires calculation of several avoided crossings on the stabilization graph which of course requires a sufficiently large basis set. Additionally, a precision of the obtained results itself highly depends on using *semi-complete basis sets*. Compared to a direct application of complex scaling on the Hamiltonian, I obtained two orders of magnitude smaller precision of the calculated complex resonance energy for the helium doubly excited resonance $2s^2$ when using the same semi-complete basis set (yet the precision up to $4 \times 10^{-5} E_h$ has been achieved).

Despite of this disadvantage I believe that the present method may be useful especially for describing laser-atom interactions typically in situations where a direct application of complex scaling of Hamiltonian would represent a technical or numerical problem.

ACKNOWLEDGEMENTS

This work was financially supported in parts by the Grant Agency of the Czech Republic (Grant No. GA20-21179S) and the Czech Ministry of Education, Youth and Sports (Grant No. LTT17015).

¹P. R. Kapralova-Zdanska, “A study of complex scaling transformation using the Wigner representation of wavefunctions,” *J. Chem. Phys.* **134**, 204101 (2011).

- ²P. R. Kapralova-Zdanska, "Dynamical control near resonances in gedanken experiments using varying projectile flux," *Phys. Rev. A* **73**, 064703 (2006).
- ³W. P. Reinhardt, "COMPLEX COORDINATES IN THE THEORY OF ATOMIC AND MOLECULAR-STRUCTURE AND DYNAMICS," *Annu. Rev. Phys. Chem.* **33**, 223–255 (1982).
- ⁴N. Moiseyev, "Quantum theory of resonances: calculating energies, widths and cross-sections by complex scaling," *Phys. Rep.* **302**, 212–293 (1998).
- ⁵B. Simon, "The definition of molecular resonance curves by the method of exterior complex scaling," *Phys. Lett.* **71A**, 211 (1979).
- ⁶C. W. McCurdy and F. Martin, "Implementation of exterior complex scaling in B-splines to solve atomic and molecular collision problems," *J. Phys. B-At. Mol. Opt.* **37**, 917 (2004).
- ⁷C. W. McCurdy and T. N. Rescigno, "EXTENSION OF METHOD OF COMPLEX BASIS FUNCTIONS TO MOLECULAR RESONANCES," *Phys. Rev. Lett.* **41**, 1364–1368 (1978).
- ⁸N. Moiseyev and C. Corcoran, "AUTO-IONIZING STATES OF H-2 AND H2- USING THE COMPLEX-SCALING METHOD," *Phys. Rev. A* **20**, 814–817 (1979).
- ⁹J. Simons, "Resonance state lifetimes from stabilization graphs," *J. Chem. Phys.* **75**, 2465 (1998).
- ¹⁰T. C. Thompson and D. G. Truhlar, "New method for estimating widths of scattering resonances from real stabilization graphs," *Chem. Phys. Lett.* **92**, 71 (1982).
- ¹¹C. W. McCurdy and J. F. McNutt, "On the possibility of analytically continuing stabilization graph to determine resonance positions and widths accurately," *Chem. Phys. Lett.* **94**, 306 (1983).
- ¹²J. S.-Y. Chao, M. F. Falcetta, and K. D. Jordan, "Application of the stabilization method to the n-2 and mg- temporary anion states," *J. Chem. Phys.* **93**, 1125 (1990).
- ¹³J. Horacek, P. Mach, and J. Urban, "Calculation of s-matrix poles by means of analytic continuation in the coupling constant: application to the 2p_g state of n₂," *Phys. Rev. A* **82**, 32713 (2010).
- ¹⁴R. Curik, I. Páidarova, and J. Horacek, *Eur. Phys. J. D* **70**, 146 (2016).
- ¹⁵G. Jolicard and E. J. Austin, "OPTICAL-POTENTIAL STABILIZATION METHOD FOR PREDICTING RESONANCE LEVELS," *Chem. Phys. Lett.* **121**, 106–110 (1985).
- ¹⁶G. Jolicard and E. J. Austin, "Optical Potential Method of Calculating Resonance Energies and Widths," *J. Chem. Phys.* **103**, 295 (1986).
- ¹⁷U. V. Riss and H. D. Meyer, "CALCULATION OF RESONANCE ENERGIES AND WIDTHS USING THE COMPLEX ABSORBING POTENTIAL METHOD," *J. Phys. B-At. Mol. Opt.* **26**, 4503–4536 (1993).
- ¹⁸U. V. Riss and H. D. Meyer, "REFLECTION-FREE COMPLEX ABSORBING POTENTIALS," *J. Phys. B-At. Mol. Opt.* **28**, 1475–1493 (1995).
- ¹⁹A. U. Hazzi, "A purely L2 method for calculating resonance widths," *J. Phys. B-At. Mol. Opt. Phys.* **11**, L259 (1978).
- ²⁰M. A. Morrison and B. I. Schneider, "Electron-molecule scattering theory: An R-matrix study of low-energy elastic e-N₂ collisions in the static-exchange approximation," *Phys. Rev. A* **16**, 1003 (1977).
- ²¹T. N. Rescigno, C. W. McCurdy, and V. McKoy, "Discrete basis set approach to nonspherical scattering," *Chem. Phys. Lett.* **27**, 401 (1974).
- ²²T. N. Rescigno, C. W. McCurdy, and V. McKoy, "Discrete-basis-set approach to nonspherical scattering. II," *Phys. Rev. A* **10**, 2240 (1974).
- ²³P. W. Langhoff, C. T. Corcoran, J. S. Sims, F. Weinhold, and R. M. Gliber, "Moment-theory investigations of photoabsorption and dispersion profiles in atoms and ions," *Phys. Rev. A* **14**, 1042 (1976).
- ²⁴O. I. Tolstikhin, "Siegert-state expansion for nonstationary systems. IV. Three-dimensional case," *Phys. Rev. A* **77**, 032712 (2008).
- ²⁵U. Peskin, R. Kosloff, and N. Moiseyev, "THE SOLUTION OF THE TIME-DEPENDENT SCHRODINGER-EQUATION BY THE (T,T')-METHOD - THE USE OF GLOBAL POLYNOMIAL PROPAGATORS FOR TIME-DEPENDENT HAMILTONIANS," *J. Chem. Phys.* **100**, 8849–8855 (1994).
- ²⁶N. Moiseyev, "THE SOLUTION OF THE TIME-DEPENDENT SCHRODINGER-EQUATION BY THE (T, T') METHOD - COMPLEX SCALED MULTIPHOTON IONIZATION DISSOCIATION RESONANCE WAVE-FUNCTIONS ARE SQUARE INTEGRABLE," *J. Chem. Phys.* **101**, 9716–9718 (1994).
- ²⁷U. Peskin, O. E. Alon, and N. Moiseyev, "THE SOLUTION OF THE TIME-DEPENDENT SCHRODINGER-EQUATION BY THE (T,T') METHOD - MULTIPHOTON IONIZATION/DISSOCIATION PROBABILITIES IN DIFFERENT GAUGES OF THE ELECTROMAGNETIC POTENTIALS," *J. Chem. Phys.* **100**, 7310–7318 (1994).
- ²⁸P. R. Kapralova-Zdanska and J. Smydke, "Gaussian basis sets for highly excited and resonance states of helium," *J. Chem. Phys.* **138**, 024105 (2013).
- ²⁹C. M. Bender and S. Boettcher, "Real spectra in non-Hermitian Hamiltonians having PT symmetry," *Phys. Rev. Lett.* **80**, 5243 (1998).
- ³⁰C. M. Bender, "Making sense of non-Hermitian Hamiltonians," *Rep. Prog. Phys.* **70**, 947 (2007).
- ³¹S. Klaiman, U. Guenther, and N. Moiseyev, "Visualization of branch points in PT-symmetric waveguides," *Phys. Rev. Lett.* **101**, 080402 (2008).
- ³²P. R. Kapralova-Zdanska, J. Smydke, and S. Civis, "Excitation of helium Rydberg states and doubly excited resonances in strong extreme ultraviolet fields: Full-dimensional quantum dynamics using exponentially tempered Gaussian basis sets," *J. Chem. Phys.* **139**, 104314 (2013).
- ³³A. Pick, P. R. Kapralova-Zdanska, and N. Moiseyev, *J. Chem. Phys.* **150**, 204111 (2019).
- ³⁴P. R. Kapralova-Zdanska, M. Sindelka, and N. Moiseyev, arXiv:1903.10383.
- ³⁵P. R. Kapralova-Zdanska, arXiv:2110.14473.